Supporting Information

For

Homeotropically-Aligned Main-Chain and Side-on Liquid Crystalline Elastomer Films with High Anisotropic Thermal Conductivities

Meng Wang,[a] Jun Wang,[b] Hong Yang,*[a] Bao-Ping Lin,[a] Er-Qiang Chen,*[b] Patrick Keller,[c,d] Xue-Qin Zhang,[a] Ying Sun[a]

[a]*School of Chemistry and Chemical Engineering, Jiangsu Province Hi-Tech Key Laboratory for Bio-medical Research, Jiangsu Optoelectronic Functional Materials and Engineering Laboratory, Southeast University, Nanjing, 211189, China*

[b]*Beijing National Laboratory for Molecular Sciences, Key Laboratory of Polymer Chemistry and Physics at the Ministry of Education, College of Chemistry and Molecular Engineering, Peking University, Beijing 100871, China.*

[c]*Institut Curie, Centre De Recherche, CNRS UMR 168, Université Pierre et Marie Curie, 26 rue d'Ulm 75248 Paris Cedex 05, France.*

[d] *Soft Materials Research Center and Department of Chemistry and Biochemistry, University of Colorado, Boulder CO 80309, USA.*

General considerations. Photoinitiator Lucirin TPO (2, 4, 6-trimethylbenzoyldiphenylphosphine oxide), benzoin dimethyl ether, acrylic acid 6-acryloyloxy-hexyl ester, pentaerythritol tetrakis(3-mercaptopropionate) (PETMP) and glyoxal bis(diallyl acetal) (GBDA) were purchased from Sigma-Aldrich. ITO conductive glasses were purchased from Kaivo Electronic components Co., Ltd. The spacers were purchased from Nano-Micro. Dichloromethane was distilled from CaH_2 under argon. Other chemical reagents were used without further purification. The liquid crystalline monomer **T6E5** was synthesized following literature protocols.[1-3] The liquid crystalline monomer **A444** (4″-acryloyloxybutyl 2,5-di(4′-butyloxybenzoyloxy)benzoate) was synthesized according to the literature.[4]

Polarized optical microscopy (POM) observations of the liquid crystalline textures of the monomers and films were performed on an Olympus BX53P microscope equipped with a Mettler PF82HT hot stage. The images were captured using a Microvision MV-DC200 digital camera with a Phenix Phmias 2008 Cs Ver2.2 software. The two dimensional X-ray scattering (2D-WAXS) experiments were performed using a Bruker D8Discover diffractometer with VANTEC 500 as a 2D detector. Corundum was used for calibration of the reflection peak positions. The diffraction patterns were recorded in the transmission mode at ambient temperature using uniaxially oriented film samples. A UV lamp (20 $mW \cdot cm^{-2}$, $\lambda = 365$ nm; LP-40A; LUYOR Corporation) was used to irradiate the samples to perform the photo-crosslinking reactions. The AC electric power was produced by a Tektronix

AFG2000-SC signal generator, and amplified by a high frequency linear amplifier (FLC ELECTRONICS AB model A800).

The thermal conductivity at room temperature was determined from the thermal diffusivity, α, density, ρ and specific heat, c. The thermal conductivity λ was calculated using the following Equation (1): [5]

$$\lambda = \alpha \times \rho \times c . \tag{1}$$

The thermal diffusivity (α) of samples the films was measured by a method based on a Laser Flash Analysis (NETZSCH LFA LFA467 NanoFlash) at room temperature in a vacuum of 0.01 Pa.[6] In this method, the sample was prepared in a round shape with a 25.4 mm diameter as the sample holder is standard with fixed size and coated with a carbon layer on the entire surface by a carbon sprayer (KONTAKT CHEMIE) to enhance the thermal contact and to prevent direct transmission of the laser flash light through the specimen. Light pulse was used as a heating source to heat surface of sample firstly, and then infrared detector was used to measure the resulting temperature rise at four different positions. Ideally, light pulse width is close to infinitesimal, the thermal conduction process inside the sample is one-dimensional heat transfer from lower surface to upper surface, implying there is no lateral heat flux, no heat loss during the test process. The thermal diffusivity is determined by analyzing the temperature-versus-time curve based on the following Equation (2):[6]

$$\alpha = 0.1388 \times d^2 \times t_{1/2}^{-1} . \tag{2}$$

In Equation (2), α is the thermal diffusivity, d is the thickness of the sample and $t_{1/2}$ is the half time of upper surface temperature rise to maximum after exposure to light pulses. Appropriate mathematical model was used to correct any deviation from ideal conditions during the actual measurement. Calculation Model “Cowan + Impulse Correction” and “In-plane + Impulse Correction” were used to modify thermal loss and calculate the thermal diffusivity in the normal direction and horizontal direction respectively.

The density (ρ) in Equation (2) is obtained according to Equation (3):

$$\rho = \frac{m}{V} \tag{3}$$

The mass (m) was available by weighing the sample using electronic precision balance. The volume (V) was determined by the superficial area and thickness of the sample. The thickness (d) was measured by a cardboard thickness detector working at specific contact area and pressure.

The specific heat capacity c was measured by a differential scanning calorimeter (DSC, NETZSCH DSC 200 F3 Maia) at the heating rate of 10 ^{o}C /min using sapphire method. Three tests including blank test, sapphire test, and sample test were carried out in turn. Firstly, the base curve of DSC was achieved by the blank test. The sapphire was selected as reference sample with known $c_{p_{standard}}$ = 0.78 J/g • K. Then the DSC curves, heat enthalpy change rate *dH/dt* as a function of time t, of the sample and sapphire were calibrated with the base curve. Comparing the DSC signal of sample with that of sapphire, $c_{p_{sample}}$ of the being tested sample can be calculated based on the following Equation 4:

$$\frac{DSC_{sample} - DSC_{blank}}{DSC_{standard} - DSC_{blank}} = \frac{c_{p_{sample}} \times m_{sample}}{c_{p_{standard}} \times m_{standard}} . \tag{4}$$

DSC_{sample}, DSC_{blank}, $DSC_{standard}$ are the ordinate of the DSC curves corresponding to the sample, blank specimen, and standard specimen, respectively; $c_{p_{sample}}$ and $c_{p_{standard}}$ are the specific heat of the sample and standard specimen, respectively; m_{sample} and $m_{standard}$ are the mass of the sample and sapphire, respectively.

Preparation of 40 μm LC cells. ITO conductive glasses were cut into squares with a length of 30 mm and ultrasonic cleaned in ethanol and distilled water for 30 min, successively. The dispenser (MUSASHI, MJET-3-CTR) smear adhesive mixed with globular spacers (40 μm) on edges of ITO glasses to make two glasses stuck.

Preparation of xMELCP films. The mixture of 95 mol% monomer **T6E5** (0.1970 g, 0.475 mmol), crosslinkers 2.5 mol% GBDA (0.0030 g, 0.012 mmol) and 2.5 mol% PETMP (0.0061 g, 0.012 mmol) and 3 wt% photoinitiator Lucirin TPO (0.0061 g), heated to 110 °C in its isotropic phase, was filled by capillarity in cells of 40 μm gap. An AC electric power (360 V, 9.0 $V \cdot \mu m^{-1}$, 1.0 kHz) was applied on the ITO regions of the cell after the filled cells were slowly cooled down at −1 °C/min to 70 °C. Subsequently, UV irradiation (365 nm, 20 $mW \cdot cm^{-2}$) initiated polymerization was carried out for 2 min to complete the fast crosslinking process. The freestanding, homeotropic aligned xMELCP films were obtained by dissolving the glass cells with 40% aqueous hydrofluoric acid solution.

Preparation of xSSLCP films. The mixture of 90 mol % monomer **A444** (0.050 g, 0.079 mmol), 10 mol % cross-linker acrylic acid 6-acryloyloxy-hexyl ester (0.002 g, 0.0088 mmol), and 1 mol % photoinitiator benzoin dimethyl ether (0.0002 g, 0.0008 mmol), heated to 100 °C in its isotropic phase, was filled by capillarity in cells of 40 μm gap. The filled cells were slowly cooled down at −1 °C·min^{-1} to 62 °C, the nematic phase of the mixture. An AC electric power (240 V, 6.0 V·μm^{-1}, 100 kHz) was applied on the ITO regions of the cell. Subsequently, UV irradiation (365 nm. 20 mW·cm^{-2}) initiated polymerization was carried out for 30 min. The freestanding, homeotropic aligned xSSLCP films were obtained by dissolving the glass cells with 40% aqueous hydrofluoric acid solution.

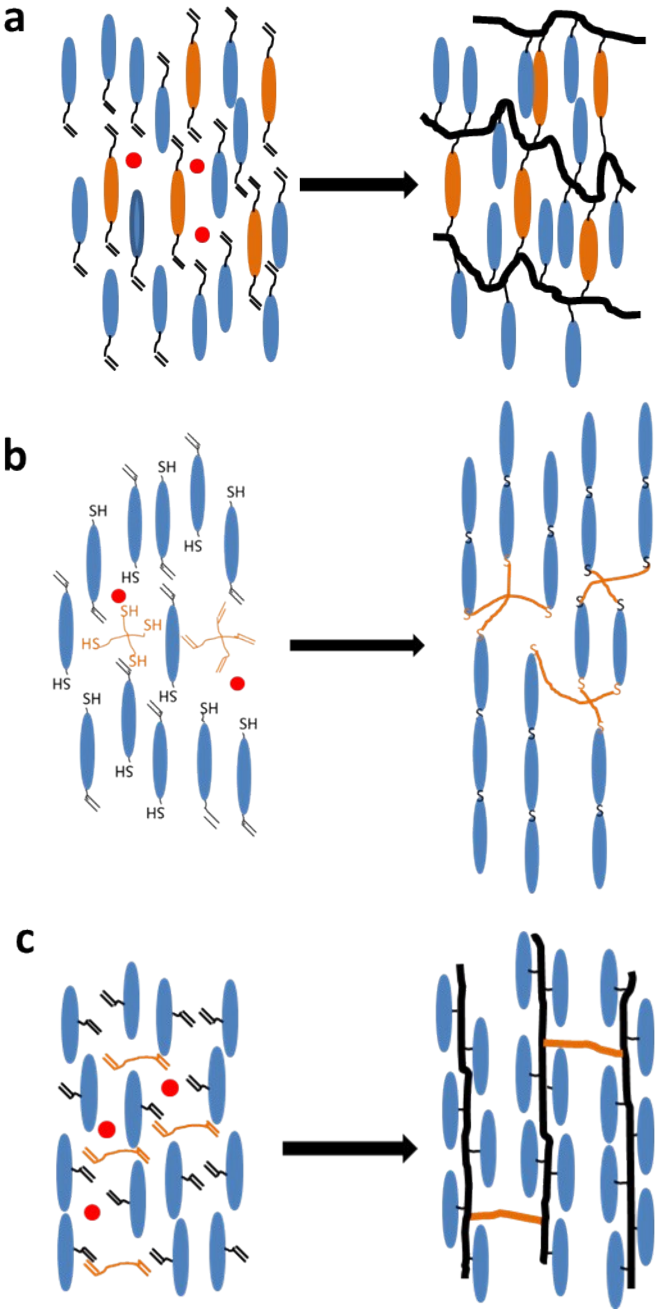

Figure S1. The schematic models of crosslinking processes. The blue, orange and red items represent the monomers, crosslinkers and photoinitiators, respectively. a) side-chain end-on system, b) main-chain end-on system, c) side-chain side-on system

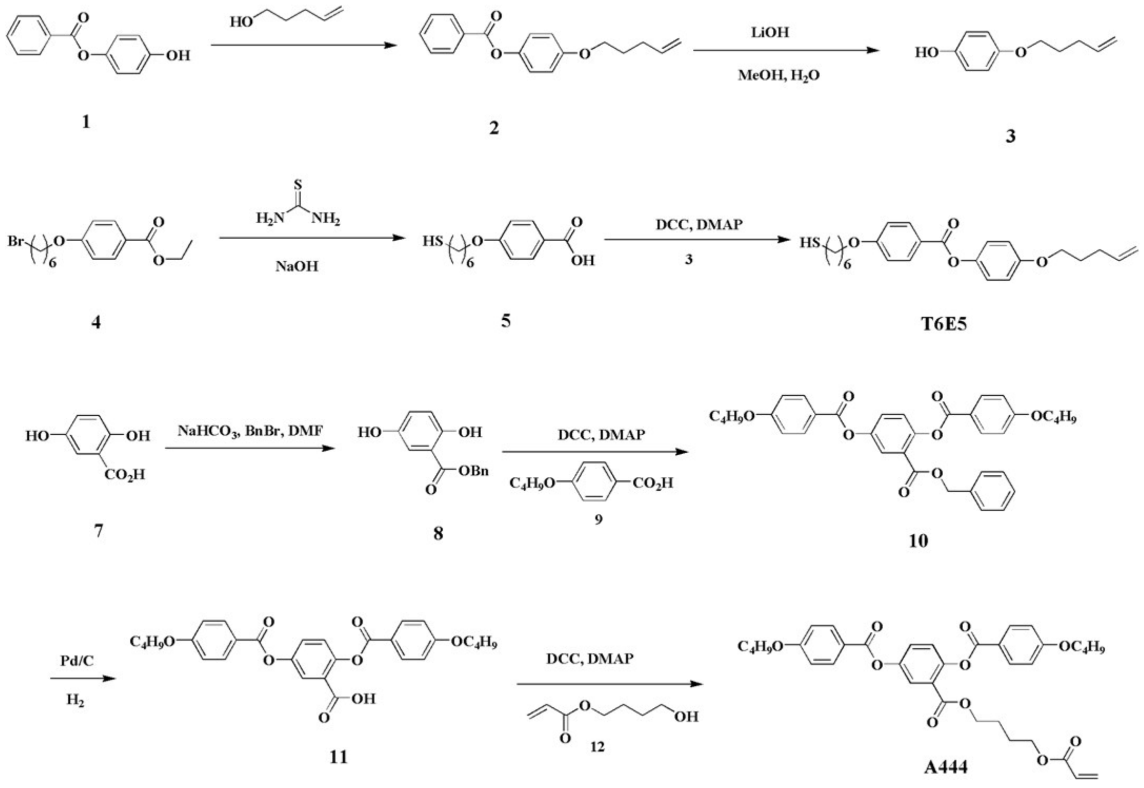

Figure S2. The synthetic routes of monomer **T6E5** and **A444**.

Synthesis and ^{1}H NMR spectra of Main-chain End-on Monomer T6E5.

The synthetic procedures were following literature protocols.[2]

Benzoic acid 4-hydroxy-phenyl ester **1** (7.83 g, 36.2 mmol), and triphenylphosphine (11.00 g, 41.9 mmol) were dissolved in 80 mL dry THF. Under a nitrogen atmosphere, 5-hexen-1-ol (3.62 g, 36.2 mmol), DEAD (6.75 mL, 41.9 mmol) were added to the mixture. The mixture was stirred overnight at room temperature and the solvent was removed in vacuum. The product was subsequently purified by flash column chromatography using silica gel as the stationary phase and a mixture of hexane and ethyl acetate, with the ratio of 20: 1, as the eluent, followed by solvent removal in vacuum to yield a white solid. The white power benzoic acid 4-pent-4-enyloxy-phenyl ester **2** was recrystallized from hexane (6.80 g, yield ratio: 67%).

Compound **2** (2.60 g, 9.20 mmol), lithium hydroxide (1.93 g, 46 mmol), methanol (60 mL) and distilled water (10 mL) were added into a 150 mL round-bottom flask. The mixture was stirred at room temperature overnight and methanol was removed in vacuum. A 2.5 M hydrochloric acid solution was slowly added into the solution until the pH was 3. The mixture was diluted with 200 mL Diethyl ether and the organic layer was washed twice with water, followed by drying over anhydrous magnesium sulfate. The colorless oil 4-But-3-enyloxy-phenol was collected as the desired product **3** (1.20 g, Yield: 80%).

Ethyl 4-(4-bromo-hexyloxy)benzoate **4** (10.00 g, 30.5 mmol), thiourea (3.48 g, 45.7 mmol) were dissolved in distilled water (6 mL), and the mixture was stirred for 2 h at 110 °C. After cooling to room temperature, the reaction mixture was diluted by

10 % sodium hydroxide solution (60 ml) and the mixture was heated at reflux for 2 h at 100 °C. The hot solution was transferred to a beaker while vigorously stirring. A 2.5 M hydrochloric acid solution was slowly added into the solution until the pH was 1. The precipitate was filtered off and the residue was washed twice using 400 ml of water. The white solid obtained was dried under vacuum at 60°C. The white power 4-(6-mercaptohexyloxy)benzoic acid **5** was collected after recrystallization from petroleum ether /2-butanone.

Compound **5** (7.60 g, 30 mmol), compound **3** (7.00 g, 42.7 mmol), DMAP (0.73 g, 4.9 mmol) and dry CH_2Cl_2 (150 mL) were added into a 250 mL round-bottom flask. Under a nitrogen atmosphere, DCC (6.47 g, 31.4 mmol) was added into the above flask in one portion at room temperature. The reaction mixture was stirred at room temperature for 12 hrs. After filtering off the solids, the reaction solution was then concentrated by rotary evaporation and the resulting crude solid was recrystallized in ethanol to give the desired product **T6E5** (8 g, Yield: 84%) as a white solid. ^{1}H NMR (300 MHz, $CDCl_3$): δ 8.12 (AA'BB', 2H), 7.09 (AA'BB', 2H), 6.91 (m, 4H), 5.84 (m, 1H), 5.04 (m, 2H), 4.04 (t, 2H, *J*=6.41 Hz), 3.97 (t, 2H, *J*=6.42 Hz), 2.55 (m, 4H), 2.23 (m, 2H), 1.85(m, 4H), 1.66 (m, 2H), 1.49 (m, 4H).

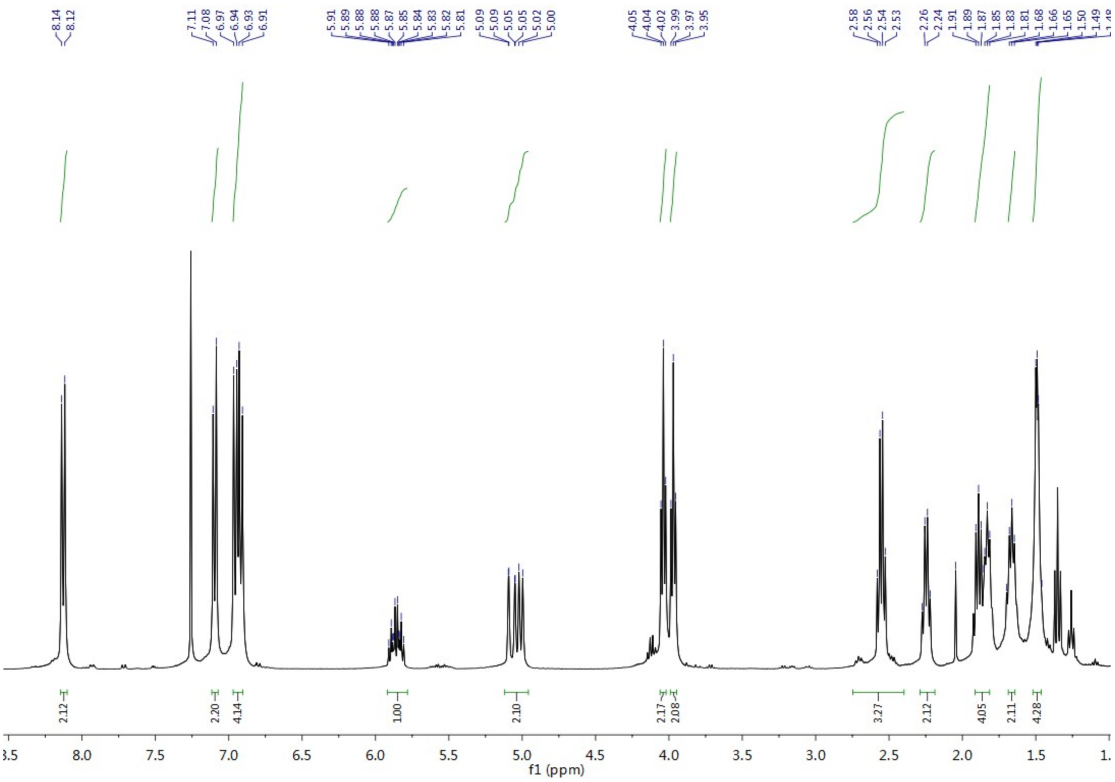

Figure S3. ^{1}H NMR spectrum of monomer **T6E5**.

Synthesis and ^{1}H NMR spectra of Side-Chain Side-on Liquid Crystalline monomer A444.

Benzyl 2,5-Dihydroxybenzoate (8). 2,5-Dihydroxybenzoic acid **7** (6.16 g, 40.0 mmol) was dissolved in dry DMF (60 mL). $NaHCO_3$ (9.90 g, 117.8 mmol) was added and the reaction mixture was stirred at 70 °C for 1 hr. Benzyl bromide (6.84 g, 40.0 mmol) were then added slowly and the mixture was stirred at 70 °C for additional 7 hrs. After cooling to room temperature, the reaction mixture was diluted with 200 mL water and extracted twice with n-hexane/ethyl acetate (1/1, 100 mL). The organic layer was washed twice with water, followed by drying over anhydrous magnesium sulfate. Then, the filtrate was concentrated under reduced pressure to give crude products. The final purification was carried out by column chromatography to give the product **8** (7.6 g, Yield: 77.7 %) as a white solid. ^{1}H NMR (500 MHz, $CDCl_3$): δ 7.47 - 7.34 (m, 5H), 7.31 (d, 1H, J = 3.05 Hz), 7.04 - 6.81 (m, 2H), 5.36 (s, 2H), 4.52 (s, 2H).

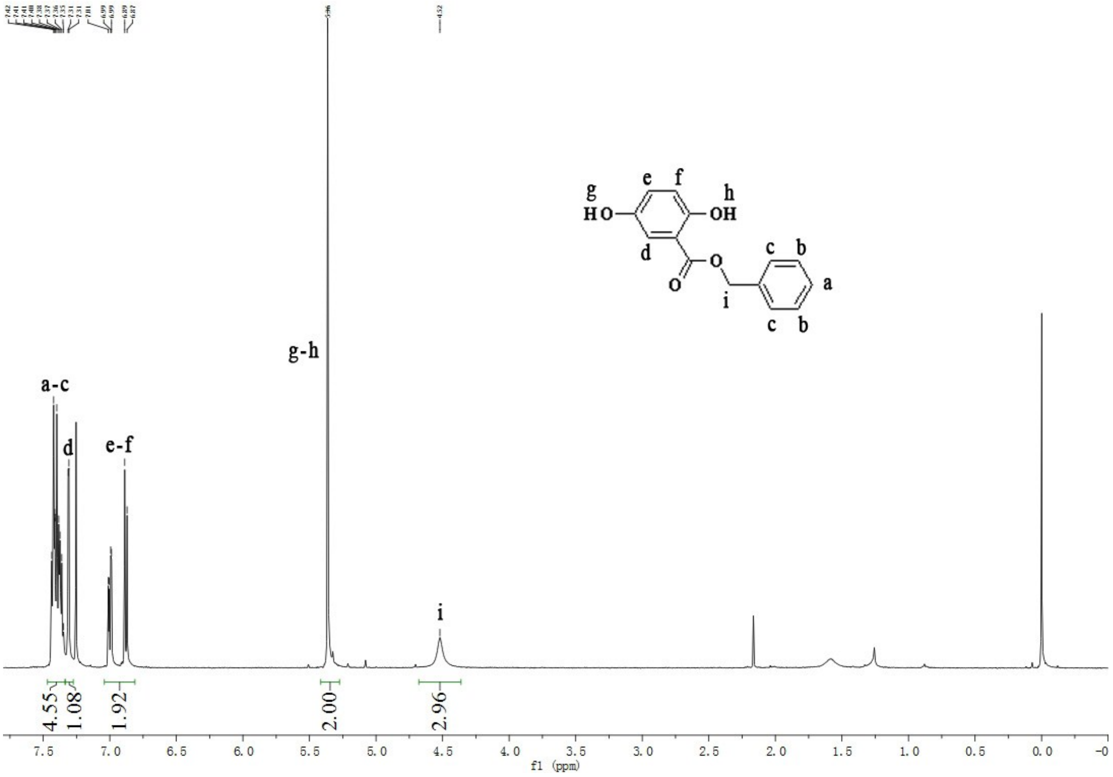

Figure S4. ^{1}H NMR spectrum of compound **8**.

Benzyl 2,5-Di(4’-butyloxybenzoyloxy)benzoate (10). 4-Butyloxybenzoic acid (**8**) (10.5 g, 54.0 mmol), compound **9** (6.0 g, 24.6 mmol), DMAP (0.8 g, 5.4 mmol) and dry CH_2Cl_2 (150 mL) were added into a 250 mL round-bottom flask. Under a nitrogen atmosphere, DCC (11.1 g, 54.0 mmol) was added into the above flask in one portion at r.t. The reaction mixture was stirred at room temperature for 12 hrs. After filtering off the solids, the reaction solution was then concentrated by rotary evaporation and the resulting crude solid was recrystallized in methanol to give the desired product (12.3 g, Yield: 84%) as a white solid. ^{1}H NMR (500 MHz, $CDCl_3$): δ 8.25 - 8.01 (m, 4H), 7.9 (d, 1H, J = 2.85 Hz), 7.26 - 7.24 (m, 7H), 7.04 – 6.86 (m, 4H), 5.19 (s, 2H), 4.06 (t, 4H, J = 6.45 Hz), 1.8 (m, 4H), 1.5 (m, 4H), 1.0 (t, 6H, J = 7.25 Hz).

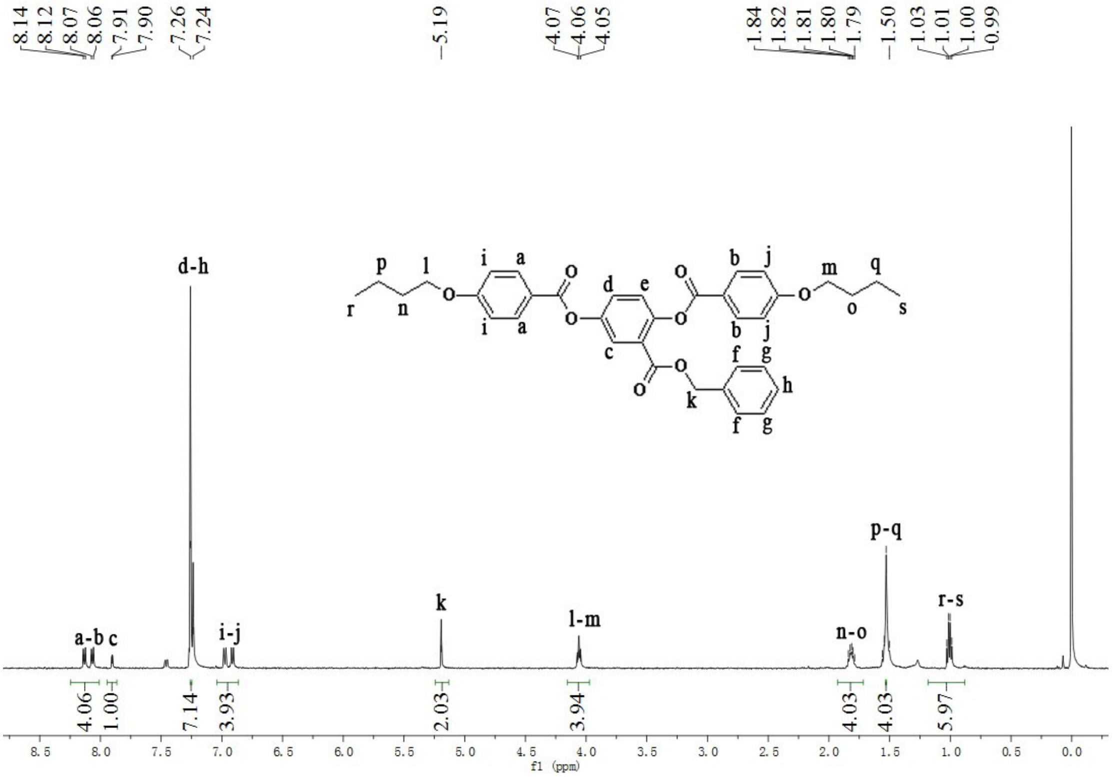

Figure S5. ^{1}H NMR spectrum of compound **10**.

2,5-Di(4’-butyloxybenzoyloxy)benzoic Acid (11). Hydrogen was allowed to bubble through a stirred suspension of 10 % Pd/C (3.0 g) in 200 mL of dichloromethane for 15 minutes. Benzyl ether **9** (12.3 g, 20.6 mmol) was added, and the reaction mixture was stirred at room temperature for 10 hrs. After filtering through a celite pad, the filtrate was concentrated, and the product (9.6 g, 92 %) was further dried under vacuum. ^{1}H NMR (500 MHz, $CDCl_3$): δ 8.23-8.07 (m, 4H), 7.9 (d, 1H, *J* = 2.85 Hz), 7.69-7.38 (dd, 2H, *J* = 8.7, 2.9 Hz), 7.04 - 6.92 (m, 4H), 4.06 (t, 4H, *J* = 3.5 Hz), 1.83 (m, 4H), 1.52 (m, 4H), 1.00 (m, 6H).

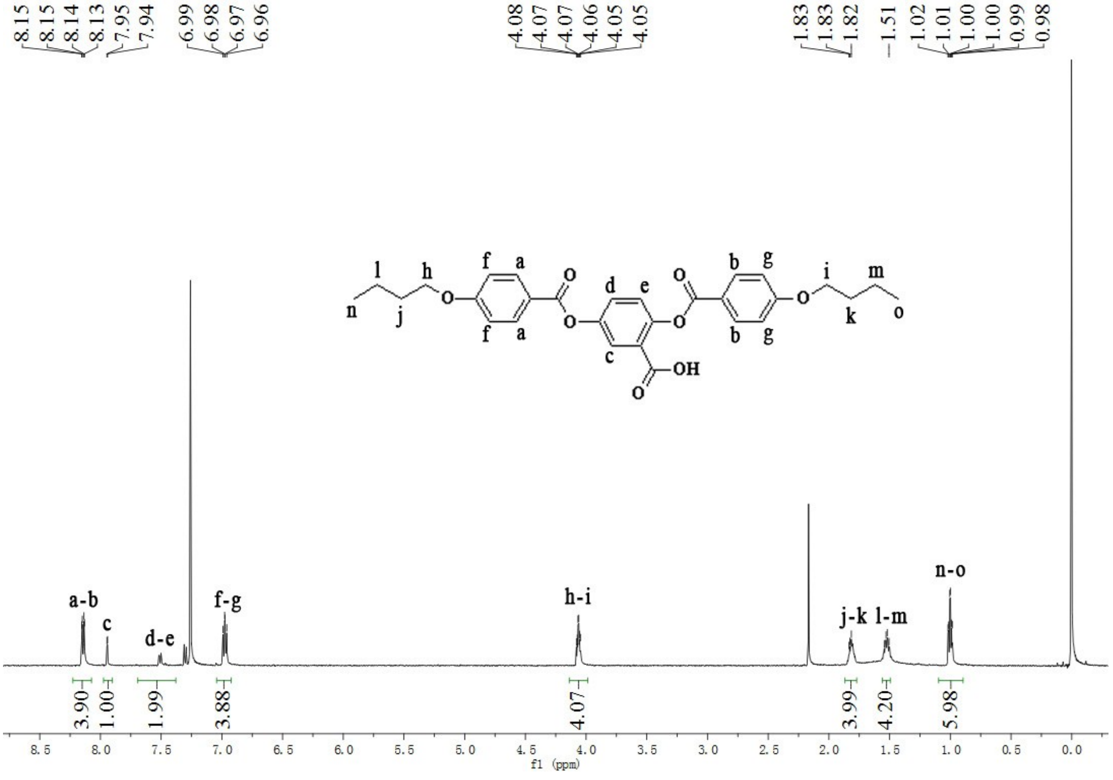

Figure S6. ^{1}H NMR spectrum of compound **11**.

2,5-Bis-(4-butoxy-benzoyloxy)-benzoic acid 4-acryloyloxy-butyl ester (A444). Compound **11** (15.18 g, 30 mmol), compound **12** (6.15 g, 42.7 mmol), DMAP (0.73 g, 4.9 mmol) and dry CH_2Cl_2 (150 mL) were added into a 250 mL round-bottom flask. Under a nitrogen atmosphere, DCC (6.47 g, 31.4 mmol) was added into the above flask in one portion at room temperature. The reaction mixture was stirred at room temperature for 24 hrs. After filtering off the solids, the reaction solution was then concentrated by rotary evaporation and the resulting crude solid was recrystallized in ethanol to give the desired product **A444** (14.22 g, Yield: 75%) as a white solid. ^{1}H NMR (500 MHz, $CDCl_3$): δ 8.23-8.07 (m, 4H), 7.9 (d, 1H, J = 2.85 Hz), 7.69-7.38 (dd, 2H, J = 8.7, 2.9 Hz), 7.04 - 6.92 (m, 4H), 6.36 (d,1H, J =8.6 Hz), 6.08 (dd, 1H, J = 8.0, 2.6 Hz), 5.79 (d, 1H, J = 8.4 Hz), 4.21 (t, 2H, J = 3.5 Hz), 4.05 (m, 6H),1.83 (m, 4H), 1.52 (m, 8H), 1.00 (m, 6H).

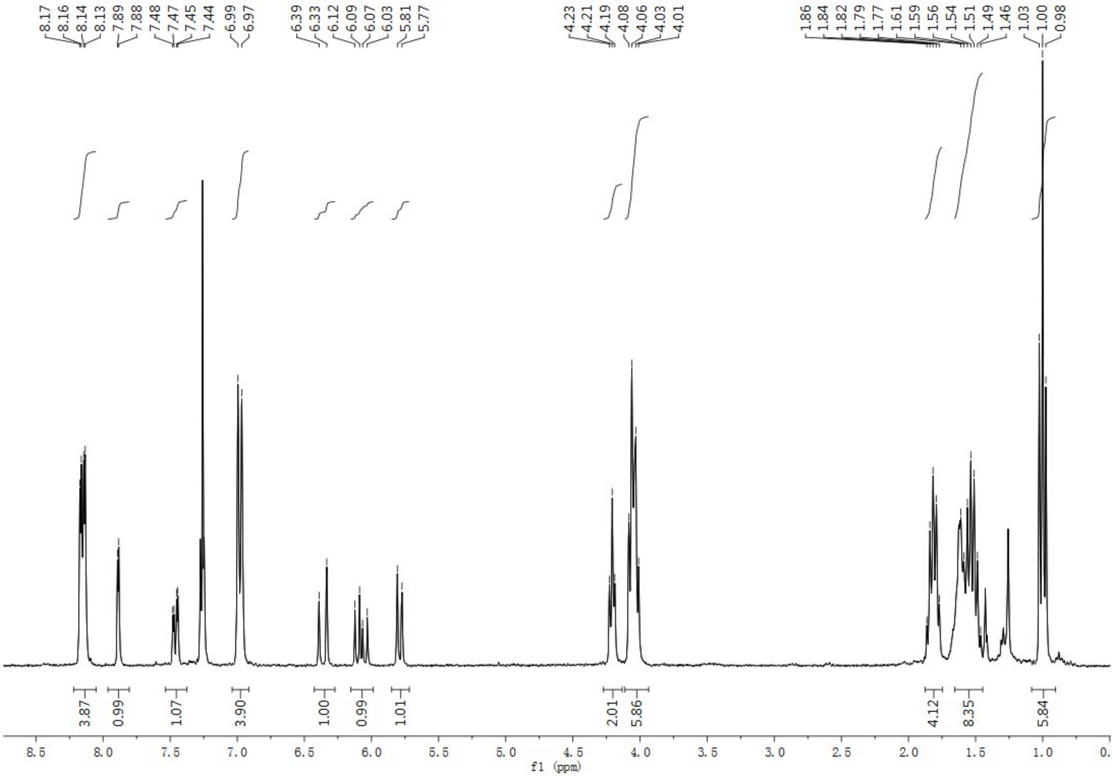

Figure S7. ^{1}H NMR spectrum of monomer **A444**.

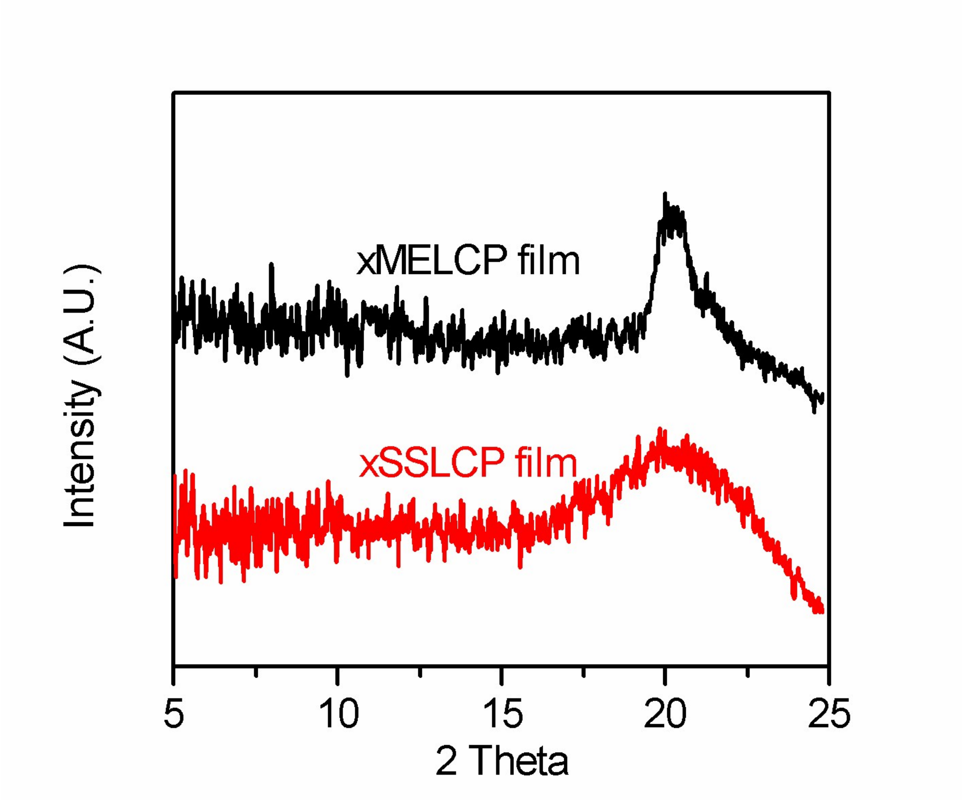

Figure S8. Scattering patterns of xMELCP and xSSLCP films in the vicinity of the outer reflection by the incident beam parallel to the film surfaces.

Figure S8 shows equatorial scans of xMELCP and xSSLCP films in the region of the outer reflection. These data are the integral of 2D-WAXS patterns along the x-axis. It is observed that the peaks of 2θ of xMELCP and xSSLCP films are at almost 20°, indicating a *d*-spacing of 4.4 Å as the space of mesogenic units. For xMELCP films, the peak centered at 20° is sharp and approximately corresponds to the crescent located in the direction perpendicular to the electric field in the 2D-WAXS pattern. Differently, for xSSLCP sample, the peak in the wide angle region is much diffused and fits reasonably with the wide-angle crescent in the 2D-WAXS pattern.

References:

1 H. T. A. Wilderbeek, M. G. M. Van Der Meer, M. A. G. Jansen, L. N. I. H. Nelissen, H. R. Fischer, J. J. G. S. Van Es, D. J. Broer, *Liq. Cryst.*, 2003, **30**, 93-108.

2 H. Yang, A. Buguin, J. M. Taulemesse, K. Kaneko, S. Méry, A. Bergeret, P. Keller, *J. Am. Chem. Soc.*, 2009, **131**, 15000-15004.

3 E. K. Fleischmann, F. R. Forst, K. Köder, N. Kapernaum, R. Zentel, *J. Mater. Chem. C*, 2013, **1**, 5885-5891.

4 D. L. Thomsen, P. Keller, J. Naciri, R. Pink, H. Jeon, D. Shenoy, B. R. Ratna, *Macromolecules*, 2001, **34**, 5868-5875.

5 C. Ortiz, M. Wagner, N. Bhargave, C. K. Ober, E. J. Kramer, *Macromlecules*, 1998, **31**, 8531-8539.

6 Q. Q. Kong, Z. Liu, J. G. Gao, C. M. Chen, Q. Zhang, G. Zhou, Z. C. Tao, X. H. Zhang, M. Z. Wang, L. Feng, R. Cai, *Adv. Funct. Mater.*, 2014, **24**, 4222-4228.